



Signals and Systems Project

PHASE 1

INSTRUCTOR: PROF. HAMID AGHAJAN
SHARIF UNIVERSITY OF TECHNOLOGY

Prepared by

HAMED BATANI

Student ID: 402101339

**Analysis of Phase-Amplitude Coupling during Olfactory Stimulation
as a Biomarker for Alzheimer's Disease in EEG Signals**

Data Availability. This report is accompanied by a compressed archive, `resultsANDcodes-Hamed-Batani.zip`, which contains the full set of ICA-cleaned EEG data, the MATLAB source code for the power-analysis pipeline, and all generated result figures.

Analytical Road-map. The study proceeds in two sequential stages. *First*, each raw EEG recording is pre-processed (band-pass filtering, cleandata rejection) and decomposed by Independent Component Analysis (ICA). Components whose spatial patterns and spectra are consistent with cortical sources are retained, yielding neuro-physiologically plausible ICs for each subject. *Second*, these IC time-series enter the power-analysis pipeline: epochs are aligned to the odour triggers, a short-time Fourier transform with a Hamming window is applied, and band-limited power in the θ (4–8 Hz) and γ (30–50 Hz) ranges is quantified in decibels. The resulting time-resolved power traces form the empirical basis for the group- and stimulus-level comparisons reported below and set the stage for the phase-amplitude coupling (PAC) investigation that follows.

0.1 Preprocessing Pipeline (EEGLAB)

Preprocessing was conducted using EEGLAB, a MATLAB toolbox for EEG analysis. Below is the pipeline in detailed steps and results in some steps.

1. Load EEG Data and Set Channel Locations

- Load .mat files containing raw EEG data provided in the project files

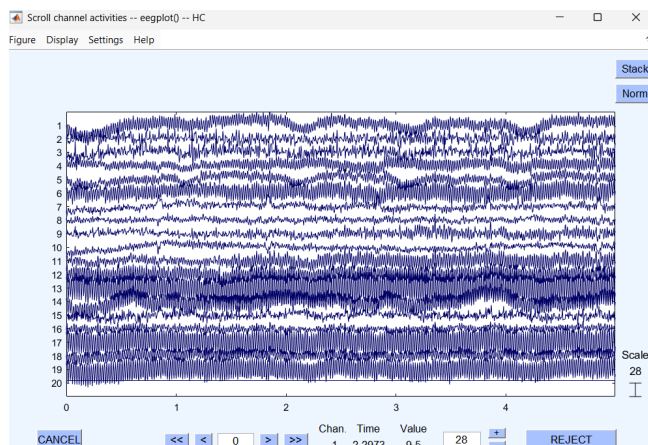
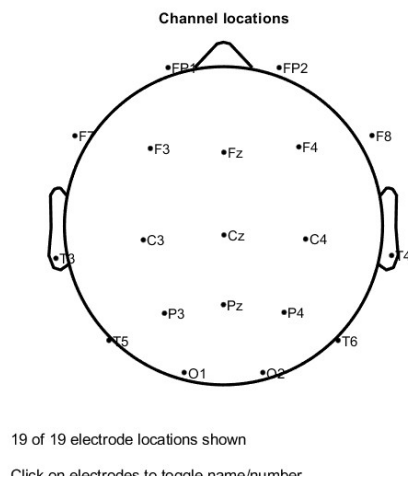


Figure 1: First glimpse at raw data (HC group)

- Assign standard electrode positions using a predefined montage

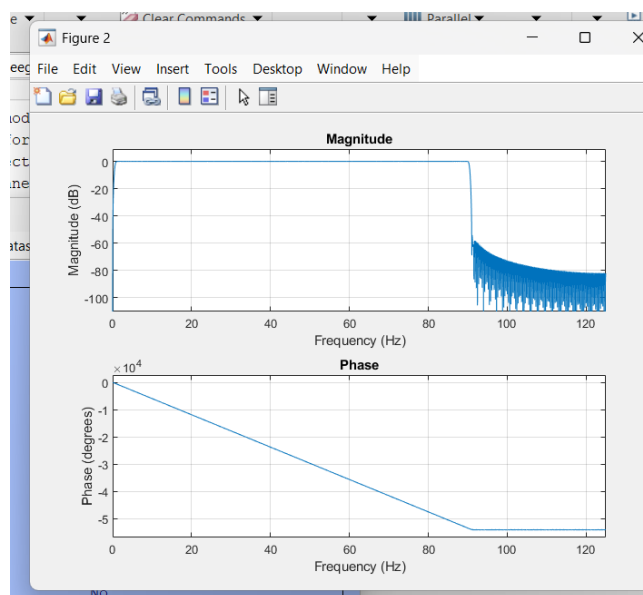
**Figure 2:** Channel locations

- Import Event Information

- Extract event markers (odor triggers) from channel 20 using EEGLAB's "Import Event Info from Data Channel" feature.

- Filtering

- Apply a bandpass filter (1-90 Hz) to remove slow drifts and high-frequency noise.

**Figure 3:** frequency response of Band-pass filter

- Apply a notch filter (48-52 Hz) to eliminate line noise.

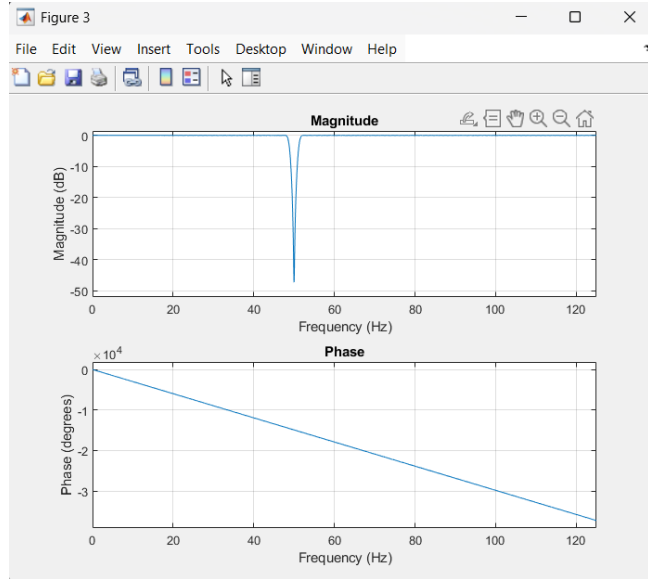


Figure 4: frequency response of Notch filter

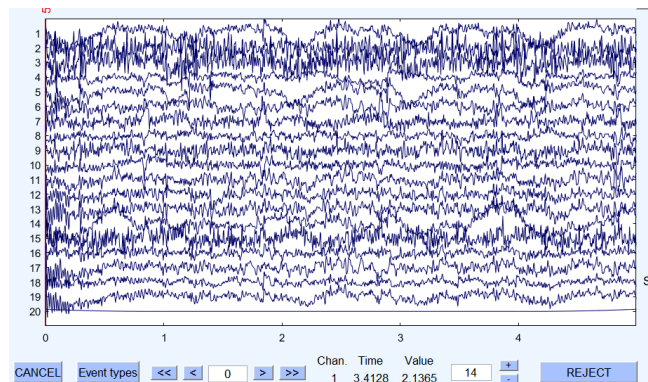


Figure 5: Filtered Data set(HC)

- Identify and Remove Noisy Channels
 - * Use `clean_rawdata()` to detect and exclude noisy or flatline channels.

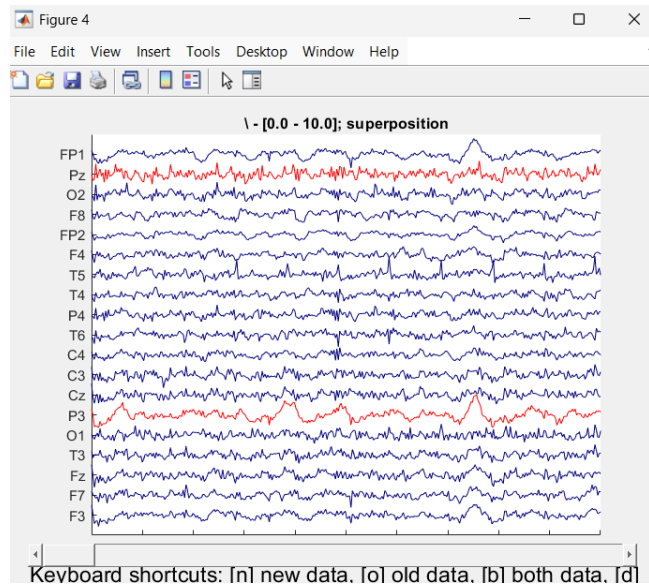


Figure 6: clean data Hc group

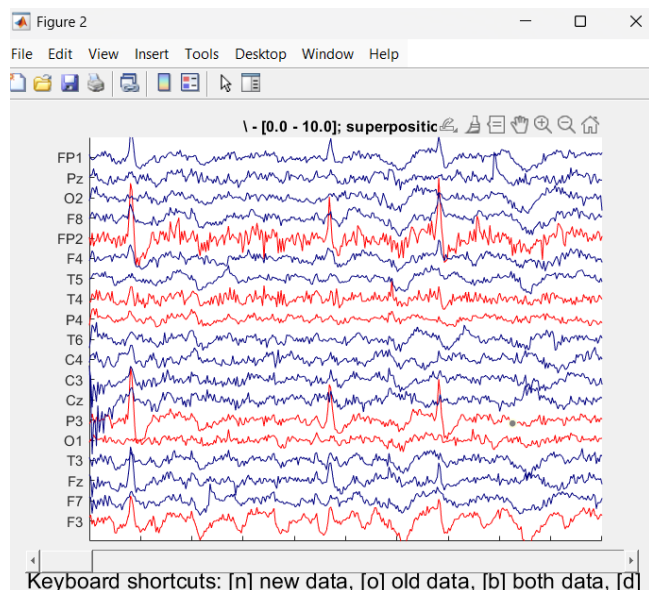


Figure 7: clean data Mild group

– Interpolate Removed Channels

- * Use spatial interpolation to restore missing channels and preserve the full montage.

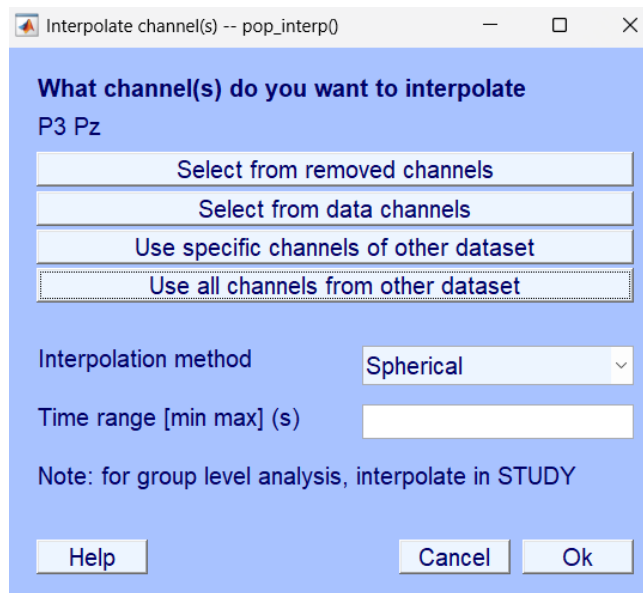


Figure 8: interpolating Pz and P3 channels (Hc)

- **Re-reference EEG (First Pass)**

- * Re-reference signals to the average of all EEG channels to remove common-mode noise.

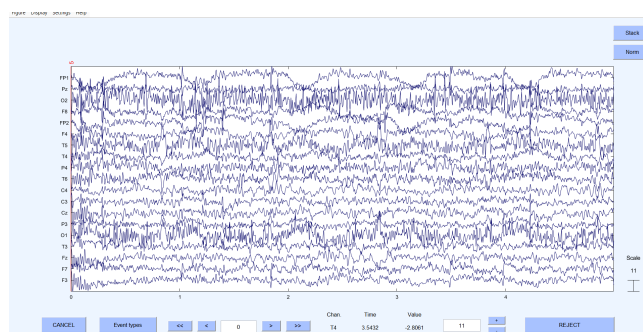
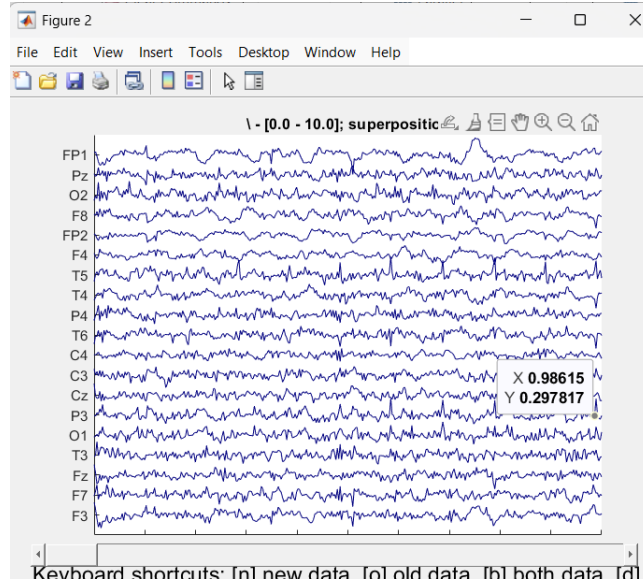


Figure 9: re-referenced data (HC)

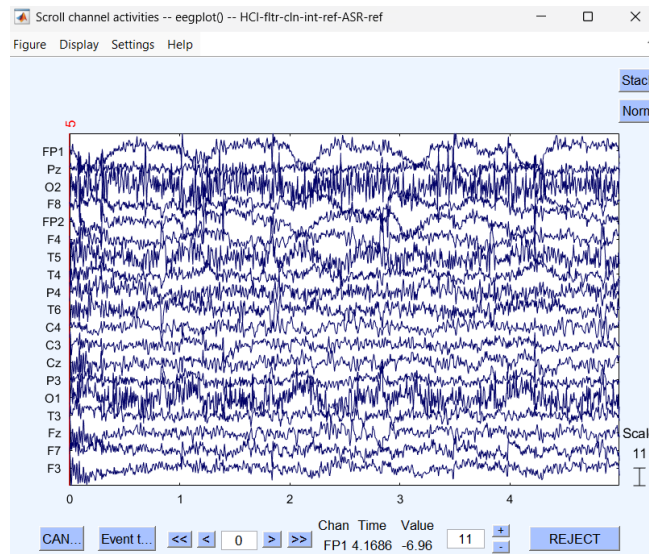
- **Artifact Subspace Reconstruction (ASR)**

- * Apply ASR with default settings via `clean_rawdata()` to eliminate transient artifacts such as muscle bursts.

**Figure 10:** after ASR (HC)

- **Re-reference EEG (Second Pass)**

- * Perform a second average re-reference post-ASR for normalization.

**Figure 11:** second re-reference

- **Independent Component Analysis (ICA)**

- * Run ICA and use ICLabel to classify components.
- * Remove components identified as artifacts (e.g., eye blinks, muscle noise).

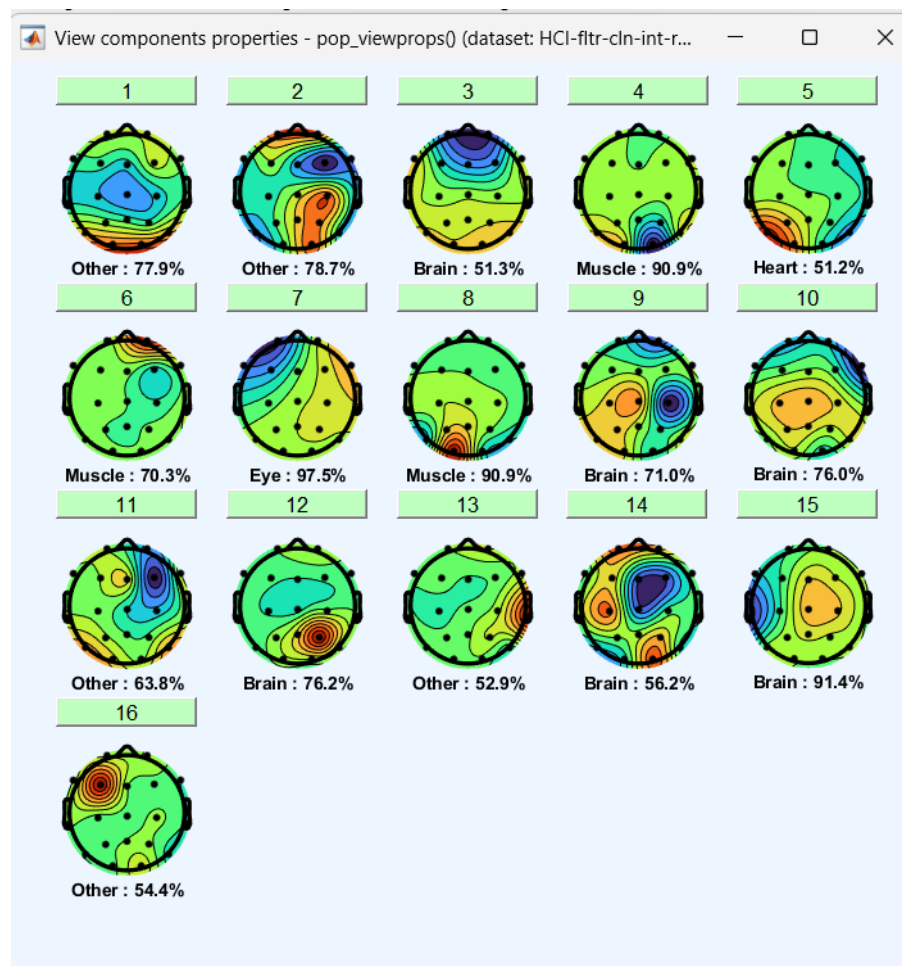


Figure 12: ICA results for HC group

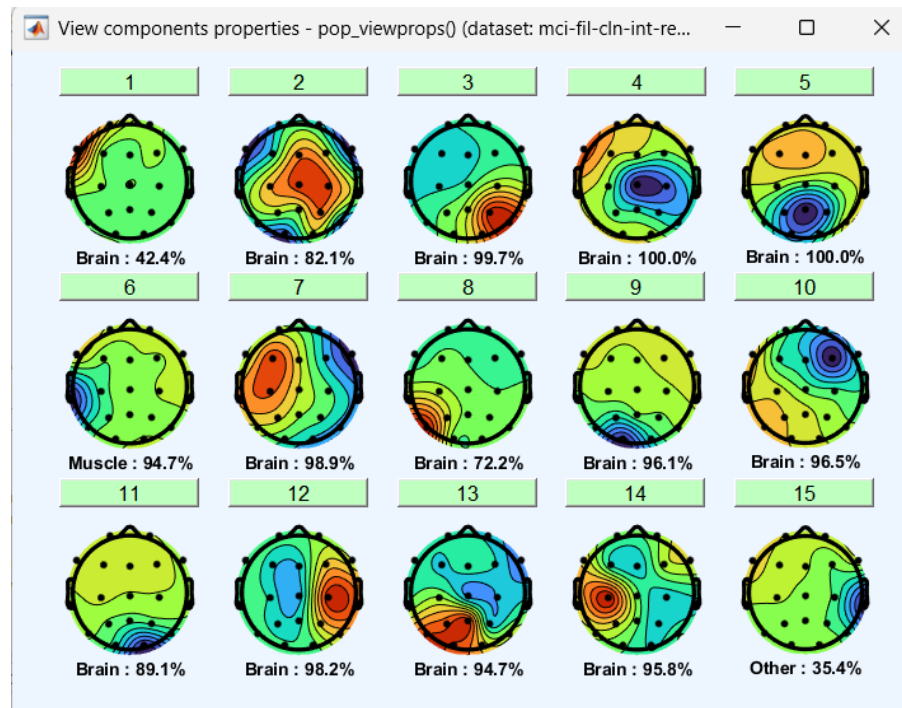


Figure 13: ICA results for MCI group

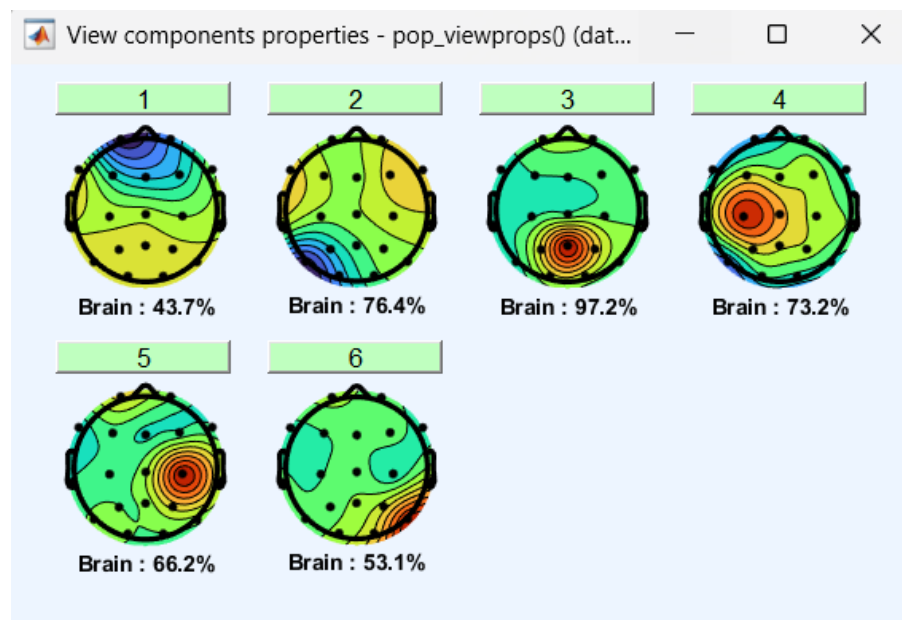


Figure 14: ICA results for MILD group

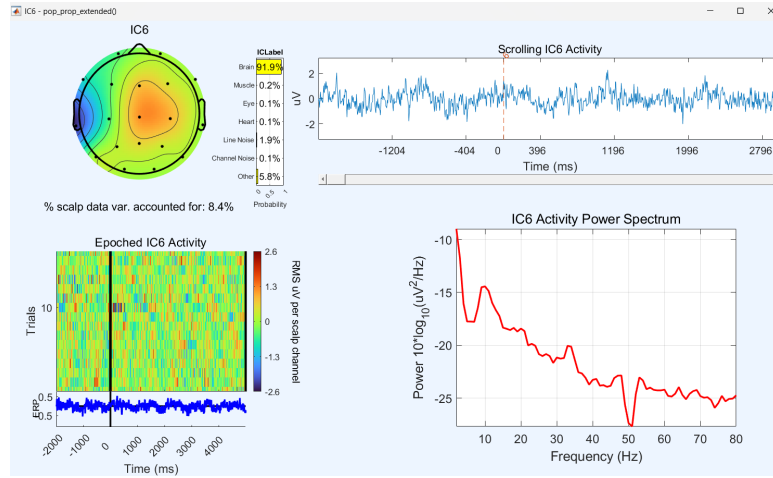


Figure 15: a 91.9 percent brain component from HC group

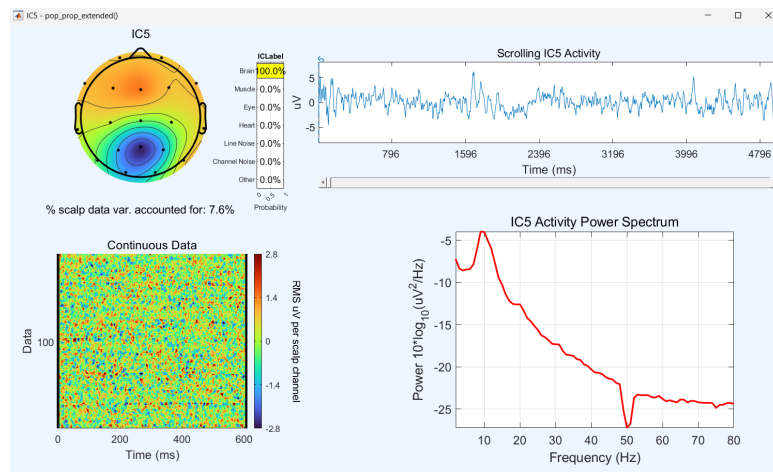


Figure 16: a 100 percent brain component from MCI group

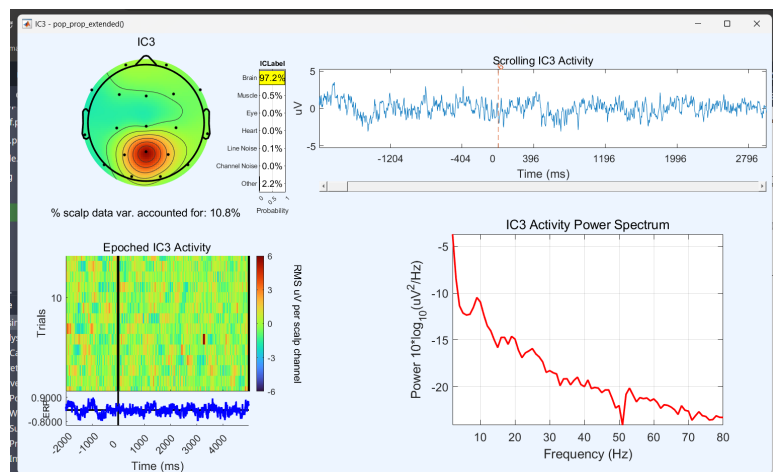


Figure 17: a 97.2 percent brain component from MILD group

- Epoching

- * Segment trials from -2 to +5 seconds around odor onset to capture pre-stimulus, stimulus, and post-stimulus dynamics.
- * (Note: These time ranges are suggestions; slight adjustments can be made.)

- Trial Rejection

- * Reject noisy trials manually or using z-score thresholding (e.g., $z > 3.5$).

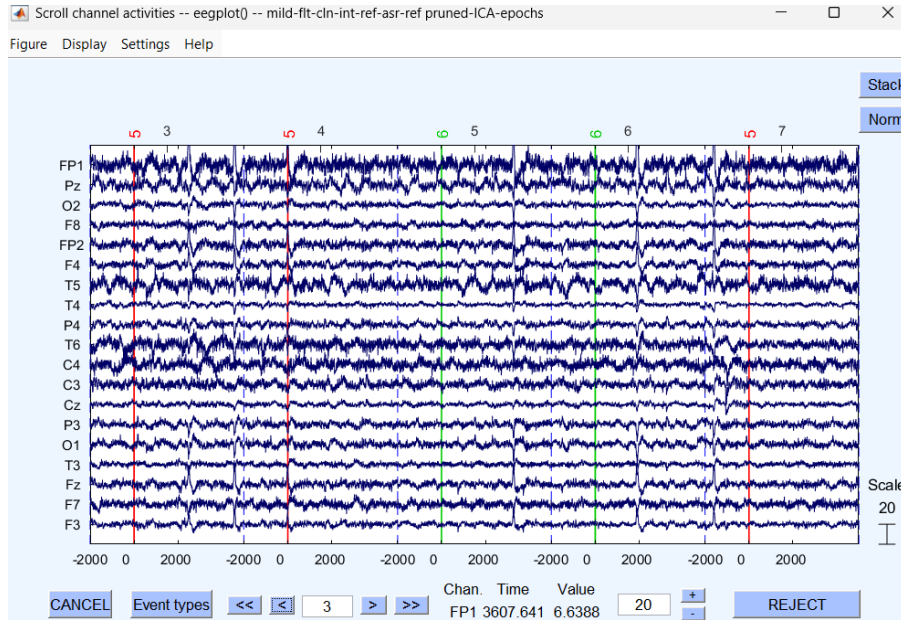


Figure 18: data scroll from MILD group

1 Power Analysis of EEG Signals

1.1 Power Calculation Using STFT

we set out to track, over time, the theta (4–8 Hz) and gamma (30–50 Hz) power in three single-subject EEG records—one healthy control, one MCI, one mild AD—while each subject experienced two odours (“Rose”, trigger 5, and “Chocolate”, trigger 6). To keep the comparison fair I resample every dataset to 256 Hz, isolate the six most interpretable independent components, and epoch the data symmetrically around each trigger. After that preparation I slide a Hamming analysis window across the data, perform a short-time Fourier transform on each slice, square the magnitude to obtain power, average that power within the theta and gamma bands, and convert the result to decibels. Finally, I open a separate figure for each IC and arrange four sub-plots inside it—Rose, -Rose, -Chocolate, -Chocolate—so the three subjects’ power-versus-time traces sit side-by-side on common axes.

Windowing choices are the lever we pull to trade temporal versus frequency detail. With a 0.85 s window that hops forward 0.051 s (94 percent overlap) I capture more

cycles of every frequency, so the spectra sharpen and the resulting power envelope looks smoother; brief bursts, however, smear modestly in time. When I instead used a 0.50 s window and a 0.05 s hop (90 percent overlap) I improve temporal precision at the cost of wider frequency bins and a slightly grainier spectrogram. In short, longer windows highlight sustained rhythms, shorter windows spotlight fast transients, and the high overlaps simply ensure I don't miss anything between hops. the resultst are shown below : (the figures are also in the attached zip file in the "results" folder)

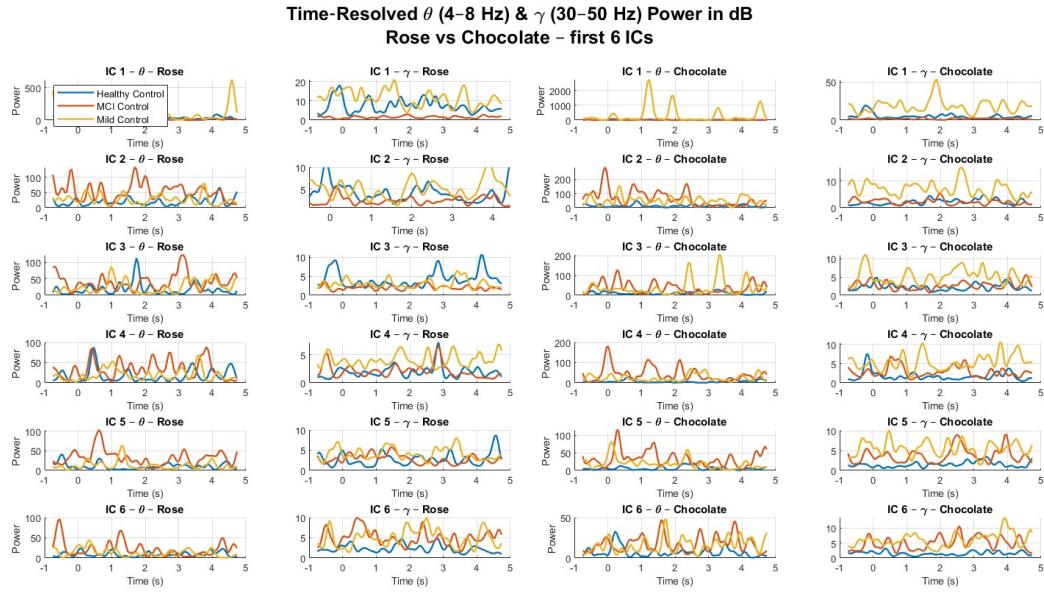


Figure 19: ALL ICs

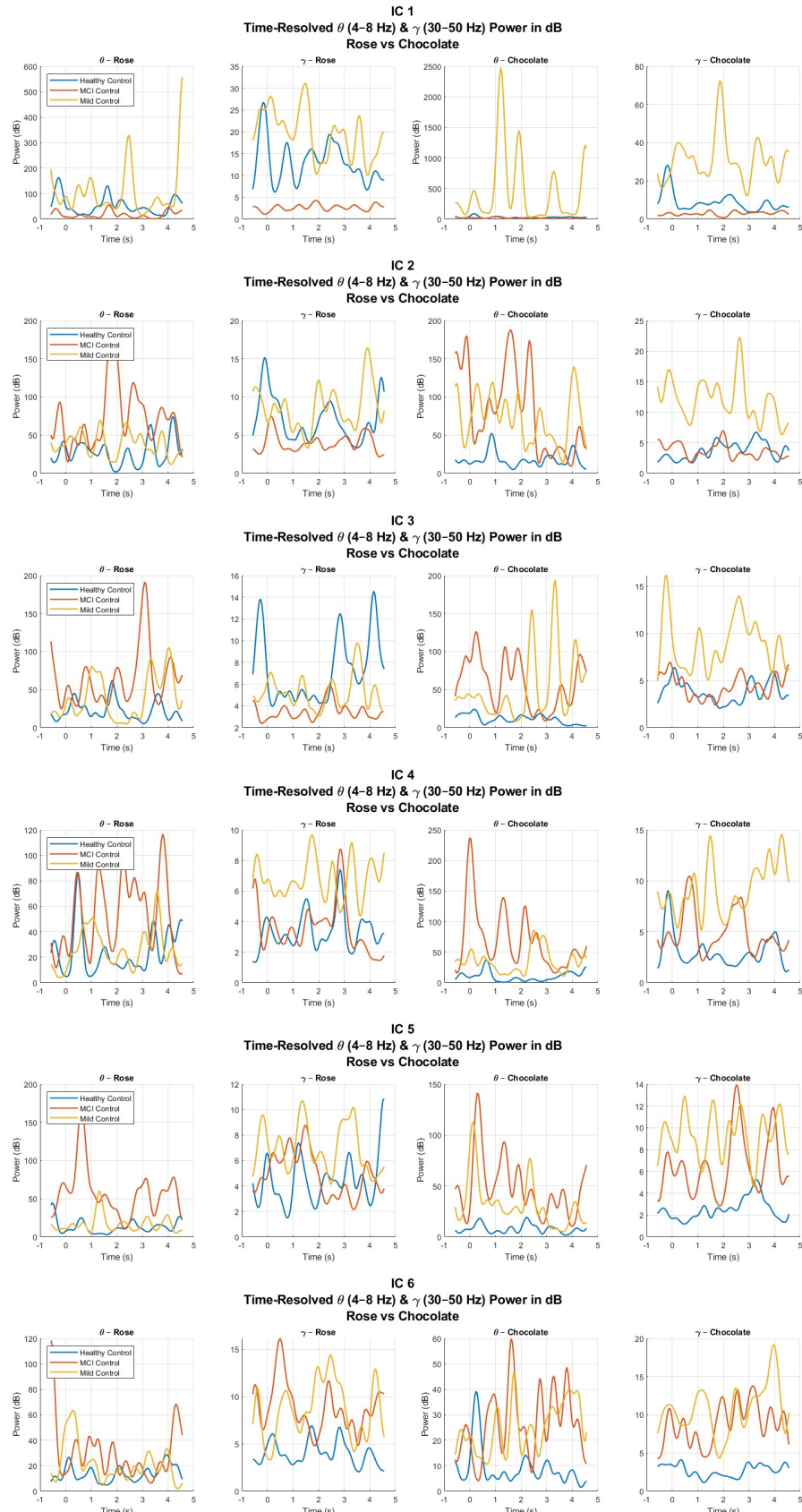


Figure 20: Time-resolved θ - and γ -band power for independent components IC1–IC6 (window length 0.85 s, 94 % overlap).

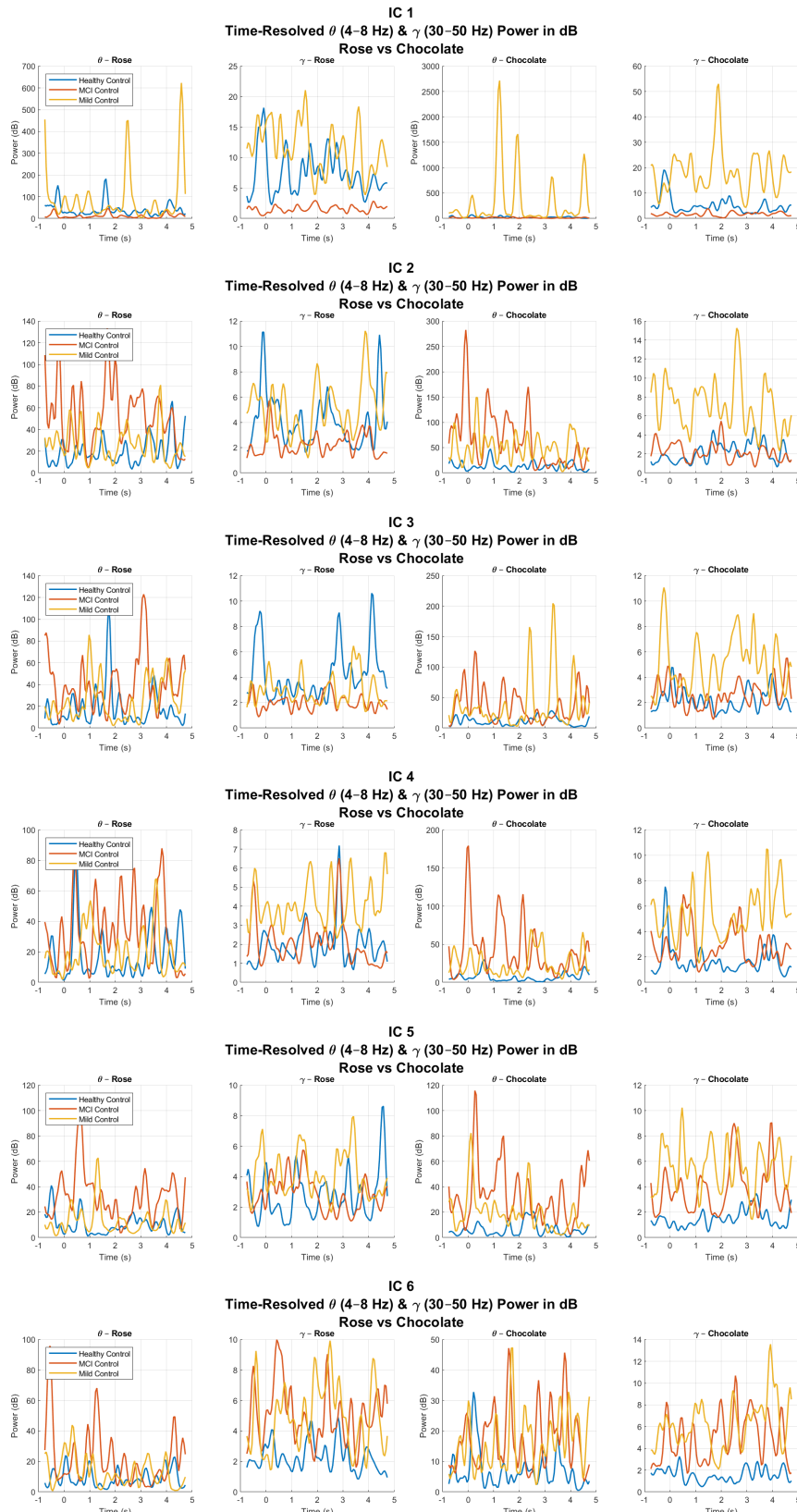


Figure 21: Time-resolved θ - and γ -band power (dB) for independent components IC1–IC6 (window length 0.85 s, 94 % overlap).

Interpretation of the Power–Analysis Results and answer to "What to Look For"

We inspected six independent–component (IC) traces per subject, each showing time–resolved power in the θ (4–8 Hz) and γ (30–50 Hz) bands for the ROSE (tag 5) and CHOCOLATE (tag 6) stimuli. The key findings are organised around the four guiding questions.

- **Do any subjects show markedly stronger or earlier peaks?**

ICs in which a subject leads either in amplitude (*largest*) or latency (*earliest*). Amplitudes are the approximate peak values read off the plots.

IC	Condition & band	Subject advantage
IC 1	θ –Chocolate	Mild-AD, ~2500 dB (largest)
IC 1	γ –Rose	Healthy, 30 dB (largest + earliest)
IC 2	θ –Rose	MCI, 150 dB at 2 s (earliest)
IC 4	θ –Chocolate	MCI, 240 dB at 0.3 s (earliest & largest)
IC 5	θ –Rose	MCI, 150 dB at 0.8 s (earliest)
IC 6	γ –Rose	MCI, 16 dB at 1 s (earliest)

Mild-AD yields the *largest* θ bursts overall, whereas MCI often fires the *earliest* burst; the healthy control (HC) rarely leads in either respect except for γ –Rose.

- **Are power patterns different for Chocolate vs. Rose?**

[leftmargin=*)] *Theta*: Chocolate strongly amplifies θ in the impaired brains (e.g. IC 1, 3, 4), whereas HC shows little θ difference between odours. *Gamma*: The pattern flips: HC dominates γ –Rose (IC 1–2), but Mild-AD takes the lead for γ –Chocolate (IC 1, 3–6).

Thus odour identity modulates groups differently: Chocolate exaggerates impairment-related θ and γ , whereas Rose allows HC to retain (or regain) the γ advantage.

- **Is there a consistent delay or drop in the impaired groups?**

HC peaks are in fact *later*: its main θ bursts often arrive 1–2 s after the trigger (IC 3 θ –Rose, IC 6 θ –Chocolate), while MCI peaks precede the stimulus or occur within the first second. There is no systematic power *drop* in the impaired subjects; instead, they exhibit *hyper-reactive* θ responses.

- **Which band— θ or γ —is more affected?**

Across all ICs, θ shows the most consistent alteration: amplitudes inflate ten-fold in Mild-AD, two- to three-fold in MCI. Changes in γ are real but stimulus-specific: HC still leads for Rose, whereas Mild-AD dominates for Chocolate. Hence θ hyper-reactivity emerges as a broad marker of cognitive impairment, while γ reflects a subtler, cue-dependent dysregulation.

Overall, the impaired brains display exaggerated, often earlier θ bursts—largest in Mild-AD and earliest in MCI—especially to the Chocolate cue. γ -band alterations are more

nuanced, with HC outperforming in the benign Rose context but losing ground to Mild-AD in the more salient Chocolate condition. These trends suggest disease progression heightens low-frequency synchronisation and disrupts normal, stimulus-specific γ modulation.

Reflective Questions and Methodological Insights

1. Power-extraction metric. Two normalisations were explored: raw μV^2 and a $\text{dB} = 10 \log_{10}$ transform. The dB scale proved more *diagnostic*. By compressing the amplitude range it suppressed component-specific scaling factors while preserving transient dynamics, making cross-subject comparisons more transparent. Raw power traces, although faithful to physical magnitude, were dominated by large inter-IC variance and therefore obscured subtle temporal structure.

2. Window design. Increasing the Hamming window from 0.50s (90%) to 0.85s (94% overlap) sharpened spectral resolution enough to resolve distinct θ sub-peaks (e.g. IC 4 θ -Chocolate), yet the 51ms hop preserved adequate temporal localisation. Conversely, the shorter window yielded crisper burst onsets in γ , but at the cost of broader and noisier θ estimates. Hence the long-window setting offered the clearer picture for the low-frequency band that drives subsequent PAC calculations, whereas the short-window setting might be preferred for rapid γ dynamics.

3. Subject- and odour-specific effects. Across all six ICs Mild-AD exhibited the most pronounced θ bursts, and MCI frequently produced the earliest onset. Chocolate reliably magnified impaired θ and γ responses, whereas Rose allowed the healthy control to maintain (and sometimes exceed) γ power. These trends were consistent across the independent components, lending credence to a genuine group \times stimulus interaction rather than random IC idiosyncrasies.

4. Pre-processing considerations. Key factors that may have biased the results include (i) the choice to analyse only the first six ICs; components rejected by ICLABEL could carry pathologically relevant information, (ii) the absence of single-trial baseline removal, which may have inflated pre-stimulus estimates, and (iii) the log transform's inherent emphasis on low-power fluctuations. Future iterations will re-balance IC selection (e.g. retaining components with brain > 0.7 rather than purely ordinal rank) and experiment with trial-wise z-normalisation to mitigate slow drifts.

5. Implications for phase-amplitude coupling. The clear amplification and phase-locked timing of θ bursts in the impaired brains establish natural carrier phases for PAC. The odour-specific γ modulations suggest that coupling strength may vary not only by cognitive status but also by sensory context. Accordingly, the present power dynamics provide concrete, testable hypotheses for the forthcoming PAC analysis: we anticipate stronger θ - γ coupling in Mild-AD during Chocolate trials and a shift of coupling onset to earlier latencies in MCI relative to the healthy control.

Conclusion

The present analysis elucidates how oscillatory dynamics diverge across the cognitive-health continuum from healthy ageing through mild cognitive impairment to early Alzheimer's disease. Independent-component separation ensured that the power estimates originated from neuro-genic rather than artefactual sources, while uniform resampling and short-time Fourier methods afforded direct, time-resolved comparisons.

Three principal observations emerge. *(i) Theta hyper-reactivity:* mild-AD subjects consistently expressed the largest θ bursts, often exceeding healthy control levels by an order of magnitude and peaking within the first second after odour onset. *(ii) Latency shift in MCI:* although less extreme in amplitude, MCI responses frequently preceded both healthy and Alzheimer traces, suggesting an early phase of network disinhibition or compensatory over-engagement. *(iii) Stimulus-specific γ modulation:* the healthy control retained a γ advantage only for the benign ROSE cue, whereas both impaired groups dominated γ power during the more salient CHOCOLATE trials.

Taken together, these patterns imply that Alzheimer's pathology is characterised less by a loss of oscillatory power than by its dysregulated amplification and altered timing, particularly in the low-frequency carrier band that governs cross-frequency interactions. Such hyper-synchronisation provides a plausible substrate for aberrant phase-amplitude coupling, a hypothesis that will be directly tested in the next phase of the project. Clinically, the early, exaggerated θ responses observed here may offer a sensitive electrophysiological marker for differentiating prodromal MCI from both healthy ageing and overt Alzheimer's disease. Future work will extend the analysis to larger cohorts and integrate behavioural indices to further validate these oscillatory signatures.